it will break first. The advantage of the architecture is evident in that the ductility increases with a corresponding increase in toughness, but there is clearly a loss in stiffness for the strand.

Conclusions

This preliminary study shows the advantages of the strand in increased toughness at the expense of loss of stiffness, a characteristic quite typical of biological structures. The "design" of the latter is such that any increase in toughness is at the cost of some reduction in stiffness. Whether man-made structures can adapt this principle is an open question but is worth further examination. In so far as use of such strandlike or ropelike fibers in composites is concerned, we continue to look into the question of behavior in compression to examine buckling and bird-caging problems. Even when those issues are resolved satisfactorily, there is of course the larger question of manufacturability. Nevertheless, the concept appears attractive and deserves further scrutiny by interested researchers.

Appendix: Governing Equations[2]

Curvatures:

$\varkappa$ = curvature with respect to x axis
$\varkappa'$ = curvatures with respect to y axis
τ = curvature with respect to z axis (twist per unit length)

Forces:

N_2 = shear force in the x direction
N_2' = shear force in the y direction
T_2 = axial force in the z direction

Moments:

G_2 = bending moment in the x direction
G_2' = bending moment in the y direction
H_2 = twisting moment in the z direction

Change in curvature:

$$\Delta\varkappa_2 = \bar{\varkappa}_2 - \varkappa_2 = 0$$

$$R_2\Delta\varkappa'_2 = R_2(\bar{\varkappa}'_2 - \varkappa'_2) = -\frac{2\sin\alpha_2\cos\alpha_2}{r_2/R_2}\Delta\alpha_2 + \nu\frac{(R_1\xi_1 + R_2\xi_2)}{r_2}\frac{\cos^2\alpha_2}{r_2/R_2}$$

$$R_2\Delta\tau_2 = R_2(\bar{\tau}_2 - \tau_2) = +\frac{(1-2\sin^2\alpha_2)}{r_2/R_2}\Delta\alpha_2 + \nu\frac{(R_1\xi_1 + R_2\xi_2)}{r_2}\frac{\sin\alpha_2\cos\alpha_2}{r_2/R_2}$$

where the barred quantities represent the state after deformation.

Normalized forces:

$$\frac{G'_2}{ER_2^3} = \frac{\pi}{4}R_2\Delta\varkappa'_2, \quad \frac{H_2}{ER_2^3} = \frac{\pi}{4(1+\nu)}R_2\Delta\tau_2, \quad \frac{T_2}{ER_2^2} = \pi\xi_2$$

$$\frac{N'_2}{ER_2^2} = +\frac{H_2}{ER_2^3}\frac{\cos^2\alpha_2}{r_2/R_2} - \frac{G'_2}{ER_2^3}\frac{\sin\alpha_2\cos\alpha_2}{r_2/R_2}$$

Total force on the strand:

$$F_t = F_1 + F_2, \quad M_t = M_1 + M_2, \quad \frac{F_1}{ER_1^2} = \pi\xi_1$$

$$\frac{M_1}{ER_1^3} = \frac{\pi}{4(1+\nu)}R_2\tau_3$$

$$\frac{F_2}{ER_2^2} = m_2\left[\frac{T_2}{ER_2^2}\sin\alpha_2 + \frac{N'_2}{ER_2^2}\cos\alpha_2\right]$$

$$\frac{M_2}{ER_2^3} = m_2\left[\frac{H_2}{ER_2^3}\sin\alpha_2 + \frac{G'_2}{ER_2^3}\cos\alpha_2 + \frac{T_2}{ER_2^2}\frac{r_2}{R_2}\cos\alpha_2 - \frac{N'_2}{ER_2^2}\frac{r_2}{R_2}\cos\alpha_2\right]$$

where m_2 = number of outer wires. Note: subscript 2 refers to outer wires.

Stress in inner wire:

Normal stress due to $F'_1 = F_1/\pi R_1^2$
Shear stress due to $M'_1 = 2M_1/\pi R_1^3$

Stress in outer wire:

Normal stress due to $T'_2 = T_2/\pi R_2^2$
Normal stress due to $G'_2 = 4G_2/\pi R_2^3$
Shear stress due to $H'_2 = 2H_2/\pi R_2^3$

Acknowledgment

The authors wish to acknowledge the assistance rendered by R. Paskaramurthy in performing the computations.

References

[1]Srinivasan, A. V., Haritas, G., and Hedberg, F. L., "Biomimetics: Advancing Man-Made Materials Through Guidance From Nature," *Applied Mechanics Reviews*, Nov. 1991, Chaps. 2 and 3.

[2]Costello, G. A., *Theory of Wire Rope*, Springer-Verlag, New York, 1991.

[3]Lee, W. K., "An Insight into Wire Rope Geometry," *International Journal of Solids and Structures*, Vol. 28, No. 4, 1991, pp. 471–490.

Some Nonlinear Response Characteristics of Collapsing Composite Shells

James M. Greer Jr.* and Anthony N. Palazotto†
Air Force Institute of Technology, Wright-Patterson Air Force Base, Ohio 45433

Introduction

AN interesting feature observed in the nonlinear numerical dynamic analysis of shells has been the appearance of chaos-like phenomena in postcollapse. Many physical systems exhibit chaotic vibrations, including the vibrations of buckled elastic structures.[1] For the purposes of definition, precollapse cases are those in which the applied load, in this case a sudden load of infinite duration, does not produce collapse; the result of the load is an oscillation of the shell structure about a deformed geometry that would have resulted had the same load been applied statically. Post-collapse refers to dynamic collapse or snap-through response. The correct choice of time step Δt is essential in nonlinear dynamic

Presented as Paper 93-1374 at the AIAA/ASME/ASCE/AHS/ASC 34th Structures, Structural Dynamics, and Materials Conference, La Jolla, CA, April 19–22, 1993; received Sept. 27, 1993; revision received March 18, 1994; accepted for publication April 8, 1994.

*Ph.D. Student, Aeronautics and Astronautics Department, AFIT/EN 522. Senior Member AIAA.

†Professor, Aeronautics and Astronautics Department, AFIT/ENY. Associate Fellow AIAA.

structural analysis, and many have suggested guidelines[2–5] for choosing a fixed time step small enough to capture the structural response. These guidelines (as those suggested herein) depend on some foreknowledge of the structure's behavior and, usually, some trial and error. Furthermore, current work suggests that using a fixed time step small enough to capture postcollapse (stiff) response is very inefficient for precollapse (soft) behavior. A number of approaches have been used in both the spatial and temporal domains for complex nonlinear problems in finite elements. Adaptive schemes have been developed for adapting the mesh, the integration order,[6] the time step as a function of location,[7,8] and timestep as a function of characteristic frequency (stiffness).[9] The scheme presented herein was developed empirically through the use of a simple shell-analog model (the subject of a future paper).

The nonlinear equations used in Dshell, an in-house finite element model, have both of the necessary ingredients for chaos[1]: 1) at least three independent dynamical variables (Dshell has seven) and 2) nonlinear terms in the coupled equations. Palazotto et al.[10] have witnessed an apparently random behavior in postcollapse states, and the present research shows that there are two sources of this behavior, one of them being chaos-like. The deformed geometries of the shell structures differ markedly depending on whether the behavior is due to chaos-like activity or numerical error. The variation of the total potential energy is used to develop the finite element for the laminated composite shell. This, coupled with the unconditionally stable integration scheme, the beta-*m* method,[2] makes energy-checking methods(for numerical stability) of little value.

Results and Discussion

A 24-ply simply supported composite cylindrical is the subject of the present research. The ply layup is $[0_6/90_6]_S$ and the material properties correspond to those of Hercules' AS4-3501-6 graphite epoxy composite. The geometry and loading of the simply supported shell are depicted in Fig. 1. The boundaries are simply supported along their straight edges, and the sudden load is applied at node 1. The static collapse load of the shell is 12,455 N(2800 lbs),

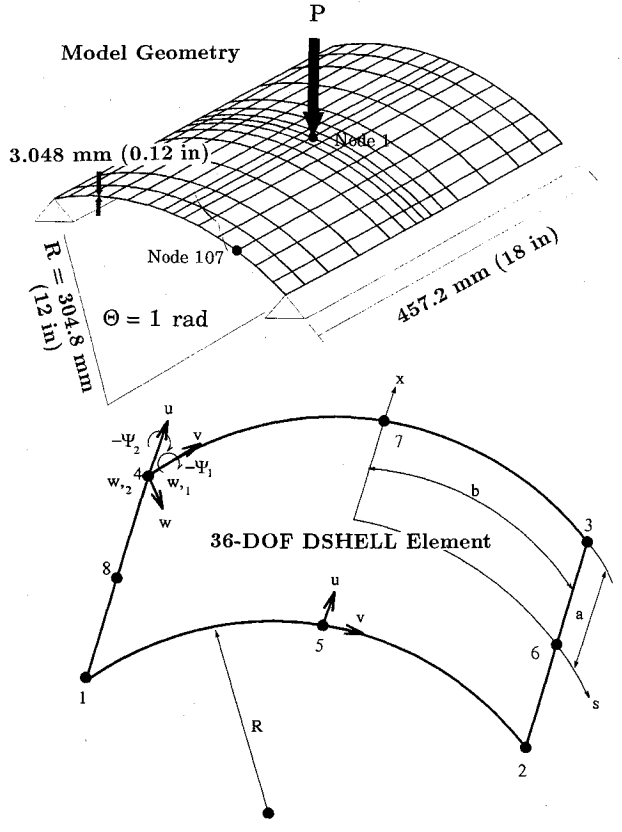

Fig. 1 Dshell model geometry and the 36-DOF Dshell element.

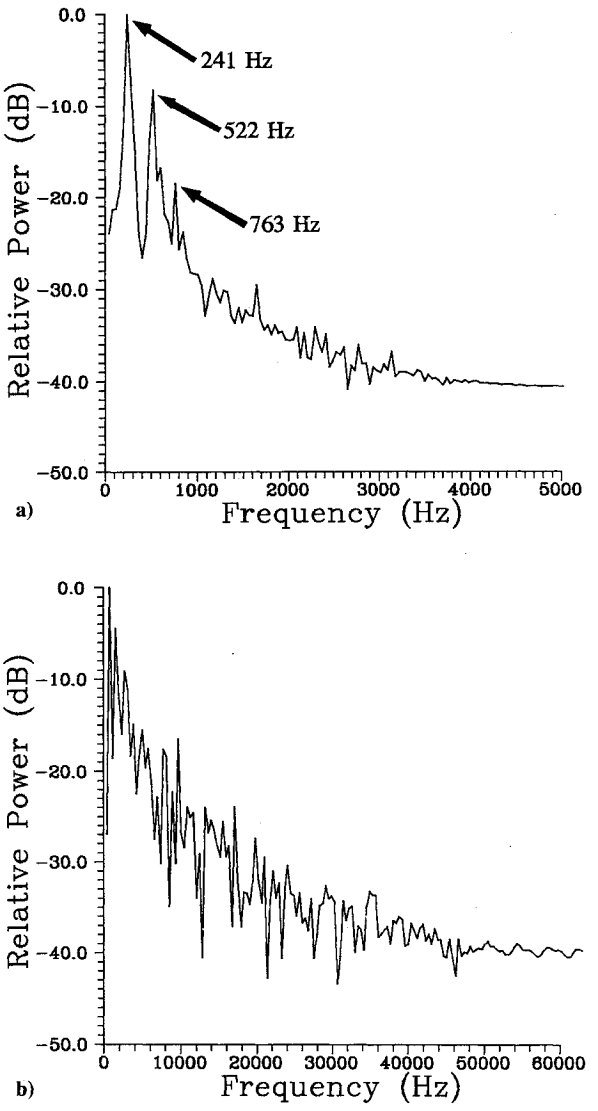

Fig. 2 Frequency response of node 1, point of applied load: a) precollapse (oscillating) and b) postcollapsed.

and was calculated using the method of Riks.[11] Only a quarter of the shell is modeled, using bilateral symmetry, which is adequate for cross-ply laminates. Two different meshes were used in the research, and both were shown to converge. The Dshell finite element is an eight-noded, 36-degree-of-freedom (DOF) isoparametric thin shell element (Fig. 1). Each corner node has seven DOF (three displacement, two slope, two rotation) and each midside node has two DOF (in-plane displacement). In-plane strains are represented by the full Green's strain displacement relation, but only linear terms are retained to describe the transverse shear strains.[12]

From previous modeling, it has been found that the integration time step for the equations of motion may be chosen based on the first linear natural frequency of the quarter-shell model, f_1

$$\tau_1 = 1/f_1 \text{ s} \tag{1}$$

$$\Delta t = \tau_1/20 \text{ s} \tag{2}$$

This empirically derived time step was found to be sufficient for all cases of precollapse motion. The frequency response of node 1 of the shell is shown in Fig. 2a for the precollapse case. The fundamental nonlinear frequency of oscillation and two harmonics are readily evident. Figure 2b is for the collapsed case (discussed subsequently).

As a first attempt at analyzing postcollapse behavior, a uniform time step of ($\Delta t = 0.00005$ s) is used in evaluating the dynamic

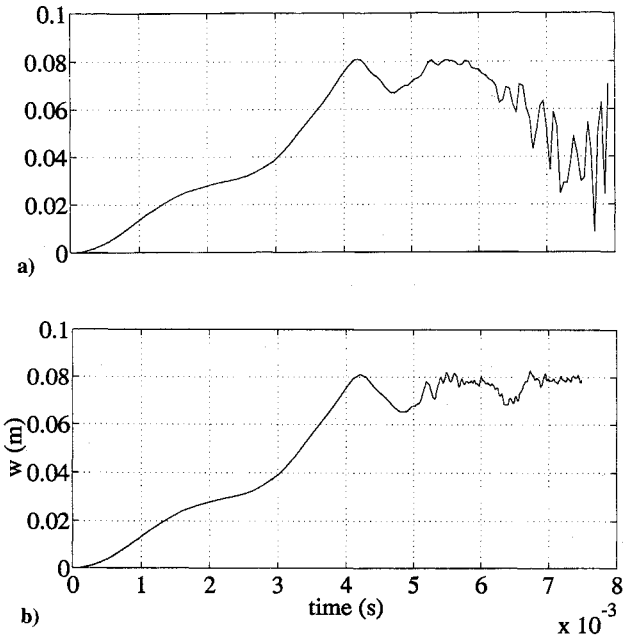

Fig. 3 Node 1 w displacement vs time: a) numerical instability with $\Delta t = 0.00005$ s and b) possibly chaotic vibration captured with two time step scheme.

snapping of the shell. The w displacement vs time is seen in Fig. 3a. Prior to collapse, the highest frequency of interest in the problem is not associated with the shell but with the suddenly applied load. If the ramping up of the load is considered to bethe first quarter of one sinusoid, the frequency of the applied load is about 125 Hz. The time step (period) of 0.00005 s corresponds to a frequency of 20,000 Hz and is smaller than necessary to capture the behavior of the sudden load and the response in the precollapse regime but is not small enough to capture the behavior after collapse. Although a cursory examination of the nodal displacement vs time(Figs. 3a and 3b) may not give an indication as to the validity of the data, the deformed geometry (Fig. 4a) gives an immediate indication that something has gone numerically wrong. Figure 4b indicates a deformed geometry in postcollapse that does not suffer from numerical error. This is not to say that this deformed geometry is realistic vis-á-vis an actual composite shell. The Dshell model does not allow any failure modes, so the collapsed geometry has features that would not be seen in an actual shell; for example, the elements spilling over the simply supported edges in Fig. 3b result from circumferentially traveling waves in the shell model that would cause large strains and failures in an actual shell and would never be observed.

The postcollapse behavior of the composite cross-ply shell was then analyzed using a multiple time step method, with otherwise identical run parameters. A time step based upon the lowest linear frequency f_1, (from the eigenvalue analysis of the quarter panel) is used during that portion of the run describing initial collapse of the shell. The high-frequency content is negligible until node 1 reaches its maximum w deflection, i.e., the shell reverses geometry and becomes very stiff. Shortly after this point (in this run, at $t = 0.0049$ s) parametric (in-plane) resonances cause the higher frequencies to become important. Hence, a postcollapse time step based on the highest frequency of interest seen in the oscillating (precollapse) shell, $f_h = 760$ Hz, is used thereafter. The highest frequency of interest was arbitrarily chosen as the highest frequency within 10 dB of the maximum (from data at the most flexible portion of the structure: the free edge). (The time necessary to generate a few cycles of oscillating behavior to get this frequency information is comparatively small compared to that required for a collapse analysis).

Using these frequencies with the criteria developed using the previously mentioned simple shell-analog model, we have

$$\tau_{\text{pre}} = 1/f_1 \approx 0.002 \text{ s} \tag{3}$$

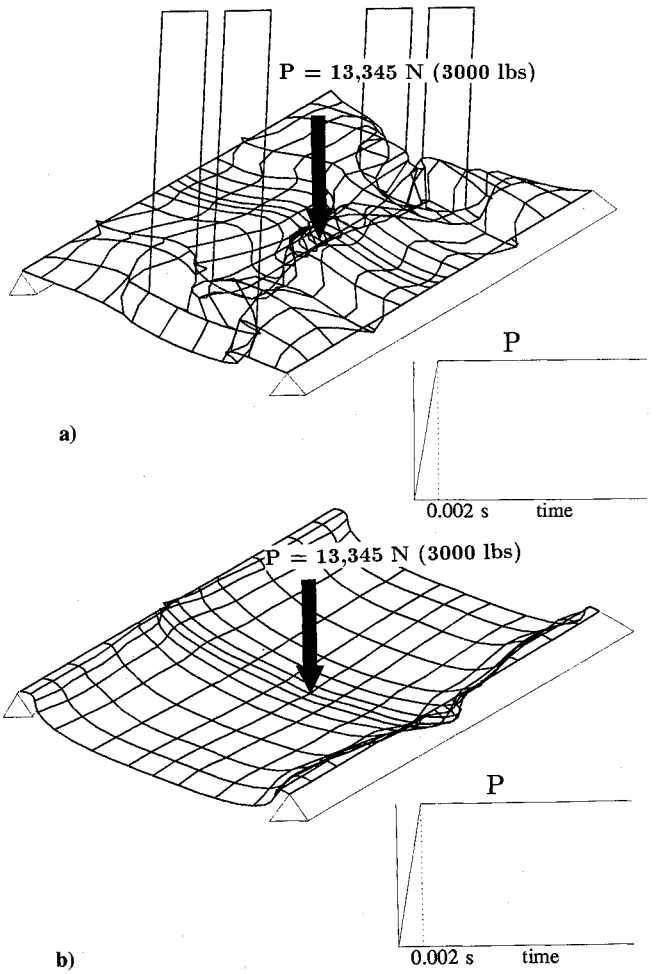

Fig. 4 Deformed geometry of postcollapse shell: a) with numerical error and b) correct deformed geometry.

$$\Delta t_{\text{pre}} = \tau_{\text{pre}}/20 \approx 0.0001 \text{ s} \tag{4}$$

$$\tau_{\text{post}} = 1/f_h \approx 0.00131 \text{ s} \tag{5}$$

$$\Delta t_{\text{post}} = \tau_{\text{post}}/160 \approx 8(10^{-6}) \text{ s} \tag{6}$$

Using Δt_{post} as the timestep for the entire run would be very inefficient; tripling the CPU time required for the solution and changing the time step during the run offers substantial improvement over using a fixed time step.

As in other schemes for nonlinear analysis, a priori knowledge of the system's characteristics is required. However, a fast Fourier Transform (FFT) analysis of a few cycles of the steady-state oscillating behavior may provide enough data to proceed with little or no trial and error. The time step for this trial run is chosen based on the linear eigenvalue analysis.

Figure 3b describes the w displacement node 1. The frequency response in the postcollapse regime is shown in Fig. 2b. It displays quantitatively the same sort of broadbanded noise seen in chaotic motion. Unfortunately, there is too little data to make a determination as to whether the motion is truly chaotic (e.g., finding a positive Lyapunov exponent).

Conclusions

For the precollapse analysis, computation of a suitable time step is straightforward and comes from the linear eigenvalue analysis. For runs involving collapse, changing the time step during the course of the run can make the run more computationally efficient.

In the precollapse cases examined, chaos-like behavior was not seen in the Dshell finite element model. In-plane displacements due to parametric resonance were found to be significant, on the order

of one-third the transverse displacements, but the high frequency content (compared to that in the postcollapse case) is negligible.

Chaos-like behavior was observed in the Dshell finite element model in postcollapse. The broadbanded frequency spectra of the oscillations and the very irregular, but bounded, nodal trajectories in phase space (not shown) are consistent with chaos.

A time step that is too small increases the number of calculations unnecessarily and hastens the accumulation of numerical error.

The deformed geometry plots give an immediate, though qualitative, indication of numerical instability whereas observation of the displacement of a single DOF vs time may not. In cases of numerical instability, Dshell is usually able to converge to a solution that satisfies compatibility and potential energy constraints although arriving at an unrealistic and incorrect deformed geometry. Unbounded trajectories in phase space also indicate numerical instability and give quantitative information as to the onset.

References

[1]Moon, F. C., *Chaotic Vibrations: An Introduction for Applied Scientists and Engineers*, Wiley, New York, 1987.

[2]Katona, M. G., and Zienkiewicz, O. C., "A Unified Set of Single Step Algorithms, Part 3: The Beta-*m* Method, A Generalization of the Newmark Scheme," *International Journal for Numerical Methods In Engineering*, Vol. 21, No. 7, 1985, pp. 1345–1359.

[3]Cook, R. D., Malkus, D. S., and Plesha, M. E., *Concepts and Applications of Finite Element Analysis*, Wiley, New York, 1989, p. 407.

[4]Almroth, B. L., Brogan, F. A., and Stanley, G. M., "User Instructions for STAGSC-1," Lockheed Missiles and Space Co., LMSC-DG33873, Vol. II, Austin, TX, Jan. 1983.

[5]Anon., "ADINA Theory and Modeling Guide," Adina R & D, Inc., Rept. ARD 87-8, Version 5.0, Watertown, MA, Dec. 1987.

[6]Toi, Y., and Isobe, D., "Adaptively Shifted Integration Technique for Finite Element Collapse Analysis of Framed Structures," *International Journal for Numerical Methods in Engineering*, Vol. 36, No. 14, 1993, p. 2323.

[7]Belytschko, T., and Lu, Y. Y., "Explicit Multi-Time Step Integration for First and Second Order Finite Element Semidiscretizations," *Computer Methods in Applied Mechanics and Engineering*, Vol. 108, Sept. 1993, pp. 353–383.

[8]Belytschko, T., and Lu, Y. Y., "Convergence and Stability Analyses of Multi-Time Step Algorithm for Parabolic Systems," *Computer Methods in Applied Mechanics and Engineering*, Vol. 102, Jan. 1993, pp. 179–198.

[9]Jacob, B. P., and Ebecken, N. F. F., "Adaptive Reduced Integration Method for Nonlinear Structural Dynamic Analysis," *Computers and Structures*, Vol. 45, No. 2, 1992, pp. 333–347.

[10]Palazotto, A. N., Chien, L. S., and Taylor, W. W., "Stability Characteristics of Laminated Cylindrical Panels Under Transverse Loading," *AIAA Journal*, Vol. 30, No. 6, 1992, pp. 1649–1653.

[11]Riks, E., "An Incremental Approach to the Solution of Snapping and Buckling Problems," *International Journal of Solids and Structures*, Vol. 15, 1979, pp. 529–551.

[12]Palazotto, A. N., and Dennis, S. T., *Nonlinear Analysis of Shell Structures*, AIAA, Washington, DC, 1992, p. 43.

Readers' Forum

Brief discussion of previous investigations in the aerospace sciences and technical comments on papers published in the AIAA Journal *are presented in this special department. Entries must be restricted to a maximum of 1000 words, or the equivalent of one* Journal *page including formulas and figures. A discussion will be published as quickly as possible after receipt of the manuscript. Neither the AIAA nor its editors are responsible for the opinions expressed by the correspondents. Authors will be invited to reply promptly.*

Comment on "Skin Friction and Velocity Profile Family for Compressible Turbulent Boundary Layers"

F. Motallebi*
Delft University of Technology, 2629 HS Delft, The Netherlands

I NOTICED the following misprints in the recent article "Skin Friction and Velocity Profile Family for Compressible Turbulent Boundary Layers"[1]:

1) In the second line after Eq. (8), $W(\eta) = 2\sin^2(\eta\Pi/2)$ should read $W(\eta) = 2\sin^2(\eta\pi/2)$.

2) Equation (10), if taken from Ref. 6, should read

$$\Pi = 0.55[1 - \exp(-0.243z_1^{0.5} - 0.298z_1)]$$

where $z_1 = Re_\theta/425 - 1$.

3) The horizontal axis in Fig. 1a is $Re_\theta \times 10^{-3}$, but in step 2 of the skin-friction algorithm it is said that "calculate $Re_{\delta 2} = \rho_e u_e \theta/\mu_w$ and find Π from Fig. 1a." Don't you think $Re_{\delta 2}$ should be replaced by Re_θ?

In addition I would like to make the following comments:

1) The title of the paper implies that the method is applicable to all zero pressure gradient compressible flows from subsonic to hypersonic flows. In the paper the method is tested mainly against hypersonic data; therefore, I think the term "compressible" should have been replaced with "hypersonic."

2) The last line in the skin-friction algorithm states that steps 1–7 are repeated until the solution converges. I am not quite sure how we can be certain of having convergence by specifying only one boundary-layer parameter (Θ or δ^*) to predict skin friction and velocity profile. More explanations were needed.

3) In step 4 of the skin-friction algorithm, the definition of U_δ^+ in relation of Eq. (6) is not clear. The addition of a clear list of notations would have been helpful.

Reference

[1]Huang, P. G., Bradshaw, P., and Coakley, T. J., "Skin Friction and Velocity Profile Family for Compressible Turbulent Boundary Layers," *AIAA Journal*, Vol. 31, No. 9, 1993, pp. 1600–1604.

Received Nov. 18, 1993; accepted for publication Dec. 30, 1993.

*Laboratory for High Speed Aerodynamics, Faculty of Aerospace Engineering, Kluyverweg 1.